International Journal of Applied Pharmaceutics

ISSN- 0975-7058 Vol 17, Issue 1, 2025

Original Article

MOLECULAR DOCKING INSIGHTS INTO PROBIOTICS *SAKACIN P* AND *SAKACIN A* AS POTENTIAL INHIBITORS OF THE COX-2 PATHWAY FOR COLON CANCER THERAPY

MOHD ABDUL BAQI[1], KOPPULA JAYANTHI[2], RAMAN RAJESHKUMAR[1*]

[1]Department of Pharmaceutical Biotechnology, JSS College of Pharmacy, JSS Academy of Higher Education and Research, Ooty, Nilgiris, Tamil Nadu, India. [2]Department of Pharmaceutical Chemistry, JSS College of Pharmacy, JSS Academy of Higher Education and Research, Ooty, Nilgiris, Tamil Nadu, India

[*]Corresponding author: Raman Rajeshkumar; [*]Email: bathmic@jssuni.edu.in

Received: 27 Aug 2024, Revised and Accepted: 26 Oct 2024

ABSTRACT

Objective: This study aims to explore the interactions between probiotics-derived bacteriocins and the COX (cyclooxygenase) pathway, particularly focusing on the cancer-associated COX-2 (cyclooxygenase-2) enzyme (PDB ID: 6COX). The goal is to assess the potential of these bacteriocins as inhibitors of COX-2, investigating their possible anti-cancer effects through modulation of this key enzyme involved in cell growth and survival pathways**.**

Methods: Using the Glide module, the study first involved the molecular docking of bacteriocins. Next, an Absorption, Distribution, Metabolism, and Excretion (ADME) study was conducted using Qikprop. The Prime Molecular Mechanics Generalised Born Surface Area (MM-GBSA) method was used to calculate binding free energy.

Results: Four bacteriocins demonstrated significant binding affinity and interactions, including hydrogen and hydrophobic bonds, with key residues such as Tyr385, Ser530, Tyr355, Arg120, Phe518, and Leu352, in the associated COX-2 enzyme(PDB ID: 6COX). Among these, *Sakacin P* exhibited an excellent XP-docking score of-6.73 kcal/mol, indicating strong binding potential. Prime MM-GBSA analysis revealed promising binding affinities with ΔBind (-90.85 kcal/mol), ΔLipo (-64.81 kcal/mol), and ΔVdW (-46.34 kcal/mol). The ligand consistently interacted with residues Tyr355, and Arg120.

Conclusion: *Sakacin P* bacteriocin, characterized by functional groups including the primary amine (NH_2), and oxygen (O), demonstrates significant potential as a COX-2 enzyme inhibitor. This suggests its promising application as an anti-cancer agent, particularly for colon cancer.

Keywords: COX-2 enzyme, Molecular docking, MM-GBSA, ADME, Cancer, Probiotics, Bacteriocins, Anti-cancer agents

DOI: https://dx.doi.org/10.22159/ijap.2025v17i1.52476 Journal homepage: https://innovareacademics.in/journals/index.php/ijap

INTRODUCTION

The COX (cyclooxygenase) pathway is crucial in the synthesis of prostaglandins, which are involved in various physiological processes, including inflammation, pain, and fever. The pathway is primarily regulated by two isoenzymes: COX-1(cyclooxygenase-1) and COX-2. COX-1 is generally expressed constitutively in most tissues and is involved in maintaining normal cellular functions such as gastric mucosal protection and platelet aggregation. In contrast, COX-2 is inducible and typically upregulated in response to inflammatory stimuli, leading to increased production of pro-inflammatory prostaglandins [1].

Dysregulation of the COX-2 pathway is commonly associated with chronic inflammation and has been implicated in the development and progression of several cancers, including colorectal cancer. Elevated COX-2 expression in tumor tissues is often linked to increased cell proliferation, angiogenesis, and resistance to apoptosis [2]. Consequently, COX-2 inhibitors have been explored as therapeutic agents for cancer, aiming to reduce tumor-associated inflammation and impede tumor growth.

Recent research has also highlighted the role of COX-2 in modulating various signaling pathways relevant to cancer, including the PI3K/AKT/mTOR pathway. Interactions between COX-2 and these pathways can influence tumor progression and response to therapy. For example, COX-2-derived prostaglandins can activate signaling cascades that contribute to cell survival and proliferation [3].

In this study, we investigate the interactions of COX-2 with the PI3K pathway, specifically focusing on the COX-2 enzyme's catalytic domain (PDB ID: 6COX). Through docking studies, we aim to understand how COX-2 may influence PI3K signaling and to explore potential therapeutic strategies for targeting these interactions in cancer treatment [4, 5].

MATERIALS AND METHODS

Molecular docking

Using molecular docking, the binding affinities and interaction processes between ligands and COX-2 enzymes were predicted. The goal was to identify the best-docked conformations based on e-model, energy, and score values. Schrödinger Suite 2021-4 was used to generate the X-ray crystal structure of the COX-2 enzyme's catalytic domain (PDB ID: 6COX. 1.65 Å resolution) fig. 1, which was obtained [6] and prepared using Schrödinger Suite 2021-4.

This preparation involved adding hydrogens, optimizing protonation states, and ensuring structural readiness for docking (Schrödinger, 2021-4). Crystallographic water molecules were removed to avoid interfering interactions [7] and missing side chains were completed using the Prime module [8]. Ligand structures were prepared with LigPrep, which generated various conformations of four bacteriocin compounds [9]. Docking simulations employed the OPLS4 (Optimized Potentials for Liquid Simulations) force field, known for its precision in modeling non-covalent interactions while maintaining computational efficiency [10]. The active site was defined using a 10 Å grid box centered on the co-crystallized ligand, which helped with the docking calculations [11]. The docking simulations were performed using Glide XP, which offers a thorough assessment of ligand binding conformations [12]. The most advantageous docked conformations were identified by evaluating the docking findings using Glide energy, score, and e-model values (Schrödinger, 2021-4). The protein-ligand complexes were visualized to analyze the interactions and conformations, as illustrated in fig. 2.

Fig. 1: The X-ray crystal structure of COX-2 enzyme's catalytic domain (PDB ID: 6COX)

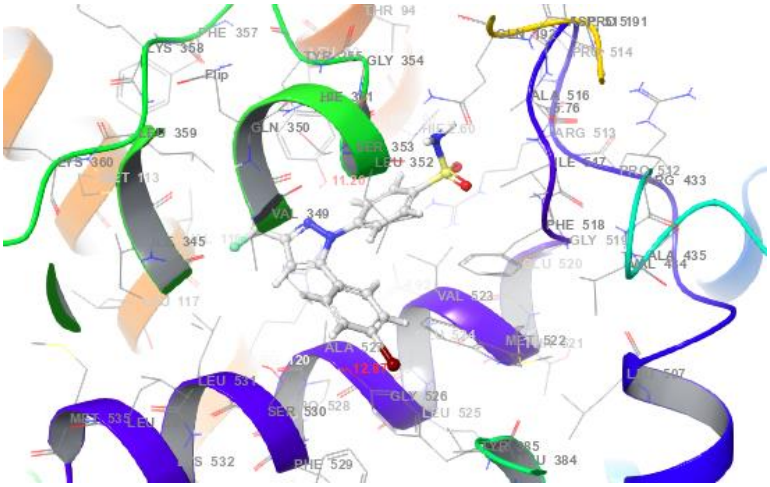

Fig. 2: Protein-ligand interaction complex (PDB id: 6COX) in molecular docking

Binding free energy calculations using prime MM-GBSA

Each protein-ligand complex's binding free energy was determined by applying the Prime MM-GBSA technique from Schrödinger Suite 2021-4. By combining different contributions to the binding free energy, this approach offers a thorough assessment of binding affinity. To calculate the binding free energy, Prime MM-GBSA blends implicit solvation models with molecular mechanics energies. The procedure entails several crucial phases, one of which is the energy minimization of every protein-ligand combination. This is accomplished by applying the OPLS4e force field, a sophisticated force field that is specifically made for modelling biomolecular interactions with great accuracy [10]. An implicit solvation model, VSGB 2.0 (Variable Dielectric Generalized Born), was used to account for solvation effects, offering a detailed treatment of hydrogen bonding, self-contact interactions, and hydrophobic effects [13]. The Surface Area Term (which accounts for the hydrophobic effect), Generalised Born Solvation Energy (which represents implicit solvation), and Molecular Mechanics Energy (which accounts for van der Waals and electrostatic interactions) are the main components that the MM-GBSA method adds up to determine binding free energy. The total free energies of the individual proteins and ligands are subtracted from the free energy of the protein-ligand complex to provide the binding energy, which is an estimate of the ligand's binding affinity to the target protein. The result of this computation sheds light on the stability and strength of the ligand-target interaction. The MM-GBSA approach also includes physics-based corrections to enhance accuracy, addressing interaction effects not fully captured by basic energy terms.

ADME calculation

The ADME (Absorption, Distribution, Metabolism, and Excretion) properties for each protein-ligand complex were assessed using Schrödinger Suite 2021-4. This evaluation involved protein-ligand systems where protein structures were sourced from experimental data or modelled as necessary, and ligands were prepared using standard molecular modeling protocols. The ADME predictions were made using the Prime QIKPROP method in the Schrödinger Suite. The OPLS4 force field was used, which is an improved version of the OPLS (Optimised Potentials for Liquid Simulations) force field. This force field is well-known for its improved performance in modelling protein-ligand interactions and its accuracy in predicting molecular properties [14]. Accurate solvation energy estimations were obtained by using the VSGB 2.0 solvation model, which successfully addressed the dynamic character of the solvent environment in protein-ligand complexes [15].

Protein and ligand structures were prepared with Schrödinger's tools, including energy minimization and protonation state assignment at physiological pH. Each complex underwent further energy minimization using the OPLS4 force field to ensure accurate low-energy conformations. The Prime QIKPROP tool then estimated ADME

properties, predicting absorption, distribution, metabolism, and excretion characteristics with high accuracy based on empirical models.

Probiotic compounds used

The study involved several bacteriocins derived from probiotic strains of *lactic acid* bacteria, which are antimicrobial peptides that inhibit the growth of similar or closely related bacterial strains. The compounds included *Sakacin A* is, a bacteriocin produced by *Lactobacillus sakei*, which is a species of *lactic acid* bacteria [16]. *Bacteriocin 28b*, from *Lactobacillus sakei*, is known for its antimicrobial activity and application in food preservation [17]. *Reuterin* is a bacteriocin produced by the probiotic bacterium *Lactobacillus Reuterin* obtained from *Lactic acid* bacteria [18]. *Sakacin P*, another bacteriocin from *Lactobacillus sakei*, is valued for its strong antimicrobial activity and use in food preservation [19]. All bacteriocins structures present in fig. 3.

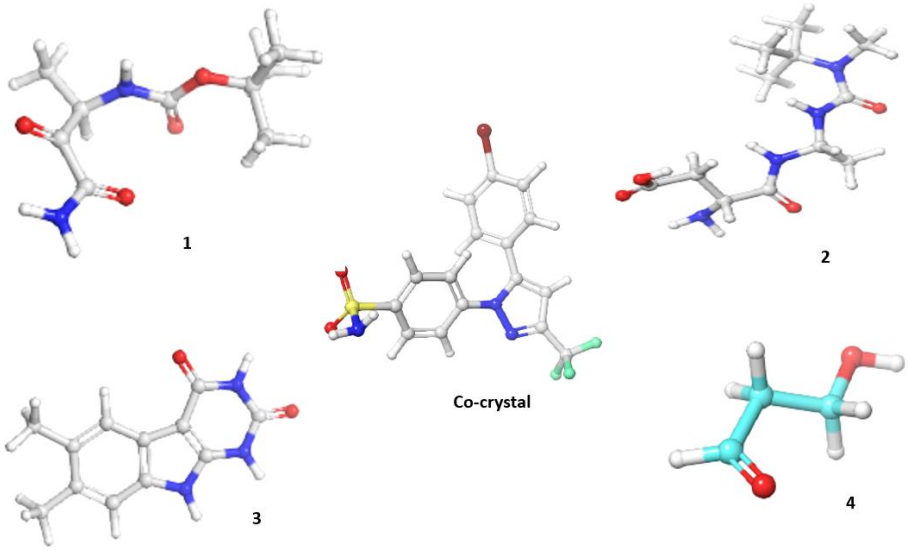

Fig. 3: Bacteriocins structures (*1). Sakacin P, (2). Sakacin A, (3). Bacteriocin 28p, (4). Reuterin*

RESULTS

Docking results and analysis

Docking studies were conducted using the COX-2 enzyme's catalytic domain crystal structure (PDB ID: 6COX) with Schrödinger Suite 2021-4. The virtual screening method based on ligands guaranteed that ligand conformations had a 1.6 Å root mean square deviation (RMSD) about the co-crystallized structure. To weed out functional groups that could have a detrimental interaction with the ligands, Lipinski's rule of five was used. Many Glide XP-docking metrics, such as the Glide score, e-model, van der Waals energy (E_vdw), Coulomb energy (E_coul), and the overall docking energy (Energy), were taken into account to assess the screening findings.

Table 1: The XP-docking scores for bacteriocins in the COX-2 enzyme's catalytic domain pocket (PDB ID: 6COX)

S. No.	Comp	[a]G_{score}	[b]G_{vedw}	[c]G_{ecou}	[d]G_{energy}	[e]G_{emodel}
1	*Sakacin P*	-6.73	-36.11	-13.82	-53.17	-30.58
2	*Sakacin A*	-5.91	-26.95	-12.82	-52.17	-29.58
3	*Bacteriocin 28p*	-4.62	-19.32	-23.37	-67.42	-27.27
4	*Reuterin*	-2.73	-18.40	-14.43	-50.51	-1.51
5	Co-crystal	-8.05	-22.52	-9.956	-31.54	-40.30

[a]Glide Score, [b]Glide E-model, [c]Glide Van der Waals Energy, [d]Glide Coulomb Energy, [e]Glide Energy.

Docking analysis revealed that all bacteriocins showed favorable binding activity compared to co-crystal, with *Sakacin P* and *Sakacin A* achieving the highest Glide scores of-6.73 kcal/mol and-5.91kcal/mol, indicating strong binding affinity. Although *Bacteriocin 28p* had a little lower Glide score of-4.62 kcal/mol than *Sakacin P* and *Sakacin A*, which indicated great binding affinities, it nevertheless demonstrated a substantial binding potential. Nonetheless, poorer binding interactions were indicated by the Glide scores of-2.73 kcal/mol for *Reuterin*. A Glide score of-8.05 kcal/mol for the co-crystal structure indicated the maximum binding affinity. Notably, *Sakacin P* also exhibited robust interaction metrics, including van der Waals energy (E_vdw) of-36.11 kcal/mol, Coulomb energy (E_coul) of-13.82 kcal/mol, total docking energy (E_energy) of-53.17 kcal/mol, and e-model (Gemodel) of-30.58 kcal/mol. These findings highlight *Sakacin P* as the most promising bacteriocin, showing binding affinity comparable to the co-crystal structure, making it a strong candidate for further research targeting the COX-2 pathway.

Binding free energy contributions using MM-GBSA

The binding free energy (ΔG_bind) contributions for every bacteriocin in complex with the COX-2 enzyme's catalytic domain (PDB ID: 6COX) are compiled in table 2 and are determined using the Molecular Mechanics Generalized Born Surface Area (MM-GBSA) technique. Coulombic energy (ΔG_Coul), hydrophobic energy (ΔG_Lip), hydrogen bonding energy (ΔG_HB), and van der Waals energy (ΔG_VdW) are among the constituents.

With major contributions from Coulombic energy (-47.42 kcal/mol), hydrophobic energy (-64.81 kcal/mol), and van der Waals energy (-46.34 kcal/mol), *Sakacin P* exhibited the greatest binding free energy of-90.85 kcal/mol, indicating considerable binding potential. With a large Coulombic energy of-60.81 kcal/mol and a smaller hydrophobic contribution of-11.64 kcal/mol, *Sakacin A* exhibited a binding free energy of-82.66 kcal/mol that was comparable. With a

positive Coulombic energy of 21.04 kcal/mol, a high hydrophobic energy of-44.19 kcal/mol, a lower van der Waals energy of-8.84 kcal/mol, and a binding free energy of-57.13 kcal/mol, *Bacteriocin 28p* has notable characteristics. Positive Coulombic energy (45.42 kcal/mol) and a moderate hydrophobic contribution (64.81 kcal/mol). The binding free energy of *Reuterin* was found to be greater at-30.85 kcal/mol in comparison to *Sakacin P*, on the other hand, the binding free energy of the co-crystal structure was recorded at-38.72 kcal/mol.

Hydrogen bonding and amino acid interactions

Table 3 presents a comprehensive overview of the hydrogen bonds that are established between every bacteriocin and the amino acid residues found in the COX-2 enzyme's catalytic domain (PDB ID: 6COX). Since they have a substantial impact on both the overall molecular interactions and the potential inhibitory efficacy of the bacteriocins, these interactions are essential for the binding affinity and stability of the corresponding protein-ligand complexes.

Table 2: Binding free energy (MM-GBSA) contribution (kcal/mol) for bacteriocins 1–4 in the COX-2 enzyme's catalytic domain complexes

S. No.	Compound code	[a]ΔGBind	[b]ΔGCoul	[c]ΔGHB	[d]ΔGLip	[e]ΔGVdW
1	*Sakacin P*	-90.85	-47.42	-4.37	-64.81	-46.34
2	*Sakacin A*	-82.66	-60.81	-1.36	-11.64	-44.73
3	*Bacteriocin 28p*	-57.13	-21.04	5.73	-44.19	-8.84
4	*Reuterin*	-30.85	-45.42	3.37	-64.81	-44.34
5	Co-crystal	-38.72	-18.09	-3.81	-13.79	-23.26

[a]Free Energy of Binding, [b]Coulomb Energy, [c]Hydrogen Bonding Energy, [d]Hydrophobic Energy (non-polar contribution estimated by solvent accessible surface area), [e]Van der Waals Energy.

Table 3: Number of hydrogen bonds and specific amino acid residues involved in bacteriocin interactions within the COX-2 enzyme's catalytic domain pocket (PDB ID: 6COX)

S. No.	Compound code	Number of hydrogen bonds	Interacting amino acid residues
1	*Sakacin P*	2	Tyr355, Arg120
2	*Sakacin A*	2	Leu352, Tyr355
3	*Bacteriocin 28p*	0	0
4	*Reuterin*	2	Tyr385, Ser530
5	Co-crystal	2	Phe518, Leu352

Each compound's hydrogen bond count and interacting amino acid residues are included in the table.

Table 3 outlines the interactions between each bacteriocin and the COX-2 enzyme's catalytic domain pocket. *Sakacin P* formed the most hydrogen bonds, with 2 interactions involving residues such as Tyr355, and Arg120. This extensive bonding indicates *Sakacin P* strong binding affinity and potential effectiveness as the COX-2 enzyme's inhibitor. *Sakacin A* established 2 hydrogen bonds with key residues including Leu352, Tyr355, and *Reuterin* formed 2 hydrogen bonds, with Tyr385, Ser530. Despite having fewer hydrogen bonds, both maintain notable interactions with the catalytic pocket. *Bacteriocin 28b* did not form any hydrogen bonds, suggesting a weaker interaction with COX-2 compared to other bacteriocins. For comparison, the co-crystal structure showed 2 hydrogen bonds with residues such as Phe518, and Leu352, reflecting well-optimized binding.

Fig. 4 displays the 2D interaction diagrams for the five bacteria strains studied, detailing their interactions within the COX-2 catalytic pocket (PDB ID: 6COX). The diagrams illustrate key interactions: Hydrogen bonding involves carbonyl groups (C=O), amines (NH_2), hydroxide group (OH) and oxygen groups (O) forming bonds with receptor residues, crucial for stabilizing the ligand-receptor complex. Hydrophobic interactions occur between non-polar groups of the compounds and the receptor's hydrophobic regions, enhancing stability. These visual representations in fig. 4 provide an intuitive view of how functional groups facilitate effective binding to COX-2, highlighting the specific residues involved in each interaction.

Fig. 5 illustrates the 3D interaction diagrams for the four bacteriocins within the COX-2 catalytic pocket (PDB ID: 6COX). The diagrams show the spatial arrangement of each bacteriocin's binding, including the binding orientation and fit within the receptor's active site. They detail how functional groups, such as carbonyls (C=O), amines (NH_2), hydroxide group (OH), and oxygen group (O), interact with receptor residues through hydrogen bonds, hydrophobic contacts, Ionic bonds. This 3D view provides insights into the molecular contacts and overall stability of the ligand-receptor complex, illustrating how these interactions influence binding and receptor function.

ADME study results

The ADME properties of the four bacteriocins were evaluated to assess their pharmacokinetic profiles and safety profiles. The results are summarized in table 4, and the following detailed explanation interprets these findings.

Table 4: ADME properties of bacteriocins and standard drug

S. No.	Compound code	CNS	SASA	Donor HB	Accept HB	QPlog P o/w	QP Caco	QPlog HERG	PSA	QPlog BB	Human oral absrtn	Rule of five
1	*Sakacin P*	-2	751.62	2	7.25	3.60	146.50	-5.17	115.23	-3.07	100	0
2	*Sakacin A*	-2	711.45	2	6.5	3.42	155.02	-5.21	86.79	-2.99	100	0
3	*Bacteriocin 28p*	-2	786.93	0	8	3.65	144.76	-5.13	124.98	-3.25	100	0
4	*Reuterin*	-1	664.43	2	6	4.16	1126.1	-5.99	81.00	-1.93	100	0
5	Co-crystal	-2	609.17	1	8.25	3.68	537.63	-4.77	115.57	-2.13	100	0

CNS: Central Nervous System Penetration (values ≤-2 indicate low CNS penetration). SASA: Solvent Accessible Surface Area (in $Å^2$), indicative of molecular surface interaction. Donor HB/Acceptor HB: Number of hydrogen bond donors and acceptors. QPlog P o/w: Octanol-water partition coefficient, indicating lipophilicity. QP Caco: Permeability across Caco-2 cell monolayers (nm/s), reflecting intestinal absorption. QPlog HERG: Potential for interaction with the HERG channel (negative values indicate lower risk of cardiotoxicity). PSA: Polar Surface Area (in $Å^2$), affecting drug permeability. QPlog BB: Blood-brain barrier permeability (negative values indicate low permeability). Human Oral Absorption: Predicted oral absorption potential. Rule of Five: Compliance with Lipinski's Rule of Five.

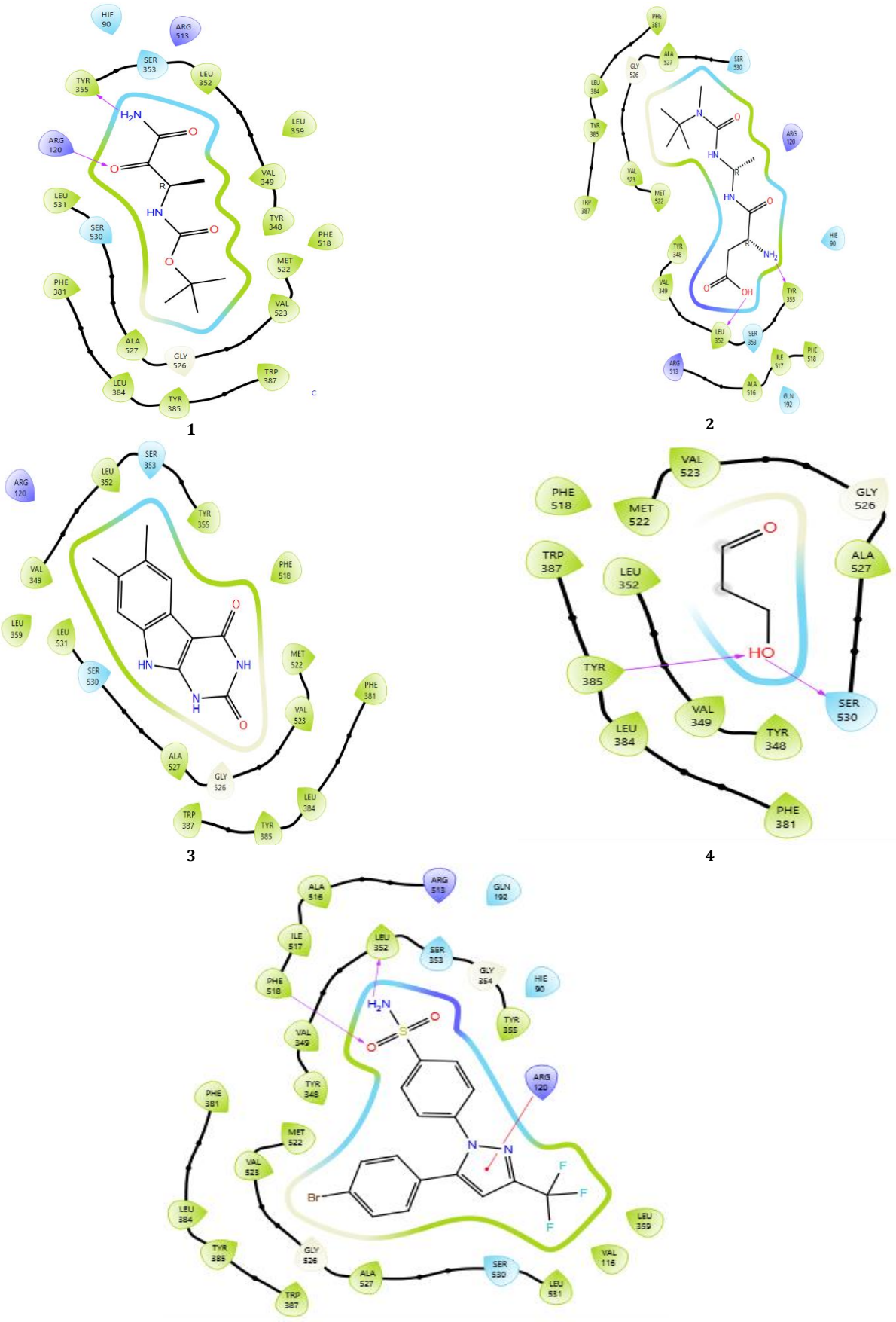

Fig. 4: Bacteriocins 2D interaction diagrams in the COX-2 enzyme's catalytic domain pocket *(1). Sakacin P, (2). Sakacin A, (3). Bacteriocin 28p, (4). Reuterin*

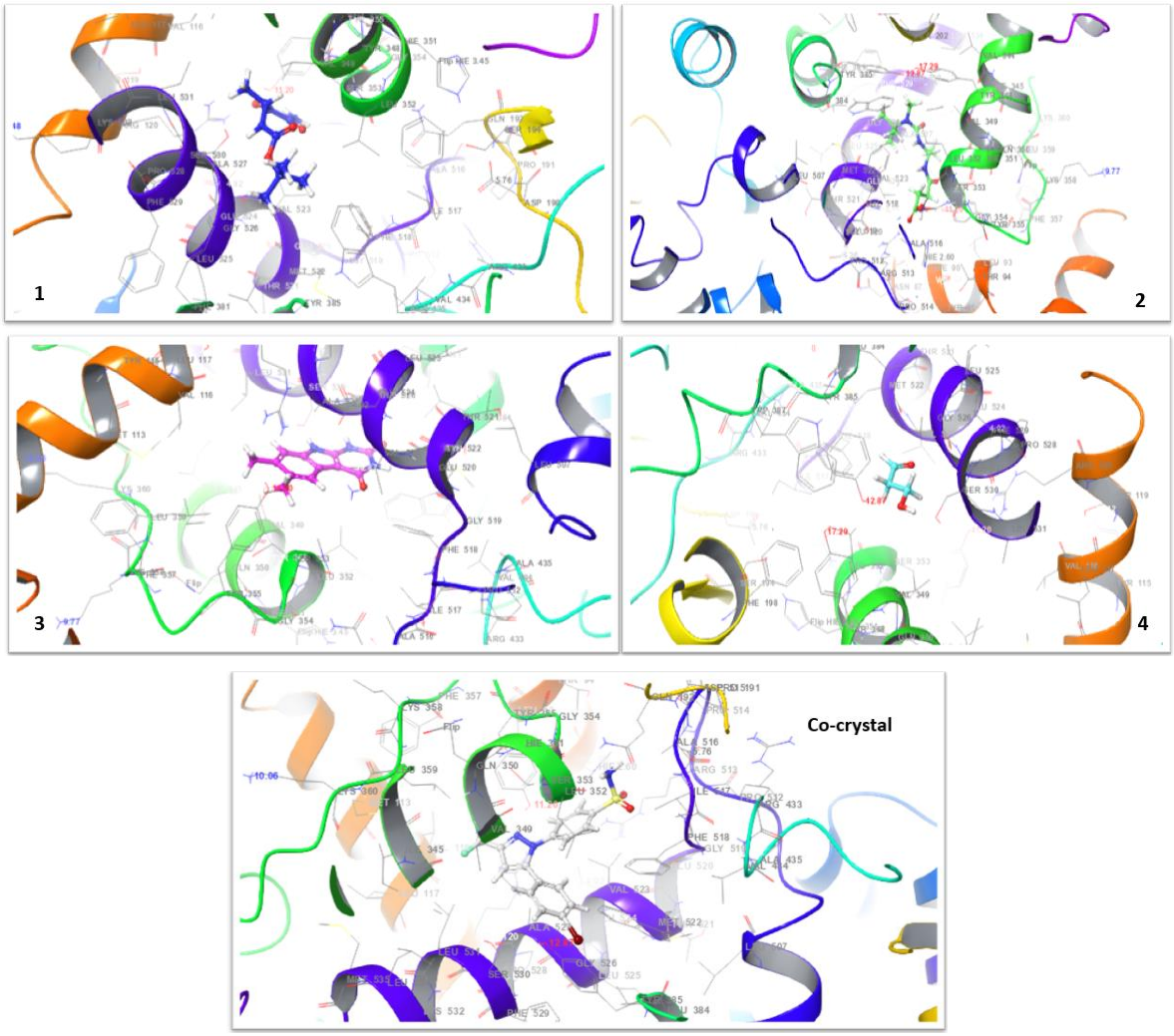

Fig. 5: 3D interaction diagrams of bacteriocins in the COX-2 enzyme's catalytic domain pocket. ***(1). Sakacin P, (2). Sakacin A, (3). Bacteriocin 28p, (4). Reuterin***

The ADME analysis reveals that all bacteriocins exhibit minimal central nervous system (CNS) penetration, with values of -2 or less, indicating a lower risk of CNS side effects. Solvent Accessible Surface Area (SASA) values range from 609.17 to 786.93 Å^2, suggesting good surface interactions and potential for effective absorption. The number of hydrogen bond donors ranges from 0 to 2, and acceptors range from 6 to 8, with *Sakacin P* and *Sakacin A* showing optimal hydrogen bonding for target interaction. Lipophilicity (QPlog P) varies from 3.42 to 4.16, indicating balanced properties for absorption. Caco-2 permeability values range from 146.50 to 1126.1 nm/s, with higher values suggesting better intestinal absorption. All bacteriocins show low cardiotoxicity risk (QPlog HERG), and negative QPlog BB values indicate low potential for crossing the blood-brain barrier. Most bacteriocins comply with Lipinski's Rule of Five, supporting good oral bioavailability. Overall, the ADME profiles suggest these bacteriocins are promising candidates for further development as safe and effective therapeutic agents.

Comparative analysis of bacteriocins and standard drug

The comparative analysis of four bacteriocins against COX-2 (cyclooxygenase-2) pathway benchmarked a co-crystal structure reveals their potential as therapeutic agents. Docking studies show *Sakacin P* and *Sakacin A* with the highest binding affinities (-6.73 kcal/mol) and (-5.91kcal/mol), outperforming others. *Sakacin P* also demonstrates the strongest binding free energy (-90.85 kcal/mol) and forms the most hydrogen bonds i. e., 2 with key COX-2 residues, indicating robust interactions. ADME properties reveal that all bacteriocins exhibit minimal CNS penetration and low cardiotoxicity risk, with *Sakacin P* and *Sakacin A* showing favorable profiles for oral absorption and lipophilicity. Despite variations in hydrogen bonding and binding free energies, these bacteriocins, especially *Sakacin P*, display promising attributes for further development as effective COX-2 inhibitors.

DISCUSSION

Molecular docking and ADME analyses highlight the promising potential of bacteriocins, particularly *Sakacin P* and *Sakacin A*, as novel therapeutic agents targeting COX-2, a crucial enzyme in cancer progression. These bacteriocins demonstrate significant binding affinities to COX-2, with docking scores of-6.73 kcal/mol and-5.91 kcal/mol, respectively, which are comparable to the co-crystal structure's score of-8.05 kcal/mol [20]. Binding free energy calculations further support their potential, with *Sakacin P* and *Sakacin A* showing free energies of-90.85 kcal/mol and-82.66 kcal/mol, respectively, indicating robust and stable interactions [21]. Extensive hydrogen bonding with key residues such as Tyr355, Arg120, Tyr385, Ser530, and Phe518 enhances their binding efficiency, suggesting a strong inhibition of COX-2 [22].

ADME profiling reveals favorable pharmacokinetic properties for these bacteriocins, including minimal CNS penetration and good oral absorption potential [23, 24]. The low cardiotoxicity risk associated with these natural compounds further supports their safety relative to conventional synthetic drugs. Notably, the probiotic origin of these bacteriocins provides an added advantage, particularly in colon cancer. Probiotics are beneficial in maintaining gut health and

modulating the gut microbiota, which can be crucial in preventing and managing colon cancer. Unlike synthetic drugs, which often come with significant side effects and toxicity, probiotics and their derived bacteriocins offer a more targeted and safer approach to treatment. They interact directly with cancer cells and contribute to a healthier gut environment, potentially enhancing overall therapeutic outcomes.

The ability of bacteriocins to target the COX-2 pathway could complement existing cancer treatments, especially for colon cancer, where maintaining a healthy gut microbiome is vital. Synthetic drugs may lack this holistic approach and can sometimes exacerbate gut issues, whereas probiotics can offer additional benefits by promoting gut health and preventing disease recurrence.

This study introduces a novel approach by investigating the therapeutic potential of bacteriocins derived from probiotics as inhibitors of the COX-2 pathway, which is crucial in cancer progression and inflammation. By identifying specific bacteriocins, such as *Sakacin P* and *Sakacin A*, that demonstrate significant binding affinity to the COX-2 catalytic domain, the research expands the application of probiotics into the realm of cancer therapy, showcasing a previously underexplored area. The rationality of this study is evident in its systematic use of docking studies to assess binding interactions, providing a solid computational basis for its hypotheses. Furthermore, investigating these bacteriocins' pharmacokinetic properties and CNS toxicity underscores careful consideration of safety and efficacy, which are essential in drug development. The focus on colon cancer, a prevalent condition often linked to COX-2 activity, aligns with the urgent need for effective treatment options. Additionally, the study's emphasis on further *in vitro* and *in vivo* research demonstrates a responsible scientific approach, ensuring that findings are rigorously validated before potential clinical application. Together, these elements highlight the study's contribution to advancing cancer therapy through innovative and well-founded research.

Future research should focus on validating these findings through detailed studies, including binding affinity assays using Surface Plasmon Resonance (SPR), molecular dynamics simulations, and comprehensive *in vitro* and *in vivo* efficacy evaluations in colon cancer models [25, 26]. Furthermore, comprehensive toxicity testing and ADME profiling will be necessary to guarantee the security and efficacy of these bacteriocins as therapeutic agents [27–29]. By integrating these bacteriocins into therapeutic regimens, particularly for colon cancer, there is potential to leverage their natural origin and multifaceted benefits, offering a promising alternative or adjunct to synthetic drugs.

CONCLUSION

This study emphasizes the potential of bacteriocins derived from probiotics as inhibitors of the COX-2 pathway, a crucial target in cancer therapy. Our docking studies identified several bacteriocins, especially *Sakacin P* and *Sakacin A*, with significant binding affinity to the COX-2 catalytic domain. These compounds demonstrated strong inhibitory potential through favorable docking scores and binding free energies. *Sakacin P*, in particular, showed the highest affinity and extensive hydrogen bonding, suggesting it is a potent inhibitor. According to Lipinski's Rule of Five, these bacteriocins have favorable pharmacokinetic qualities and minimal CNS toxicity, as shown by the ADME investigation. This safety profile suggests that probiotic-derived bacteriocins could be a safer alternative to synthetic drugs, reducing side effects. Importantly, considering the role of the COX-2 pathway in colon cancer, these bacteriocins offer a novel and potentially safer approach to targeting this pathway in colon cancer therapy. In summary, our findings support the use of these natural compounds in colon cancer therapy, highlighting their promise as effective and safer alternatives to traditional synthetic drugs. To verify the therapeutic effectiveness and safety of these findings, more research should be conducted both *in vitro* and *in vivo*.

ACKNOWLEDGMENT

The authors would like to thank the Department of Pharmaceutical Biotechnology and Pharmaceutical Chemistry, JSS College of Pharmacy, Ooty, Tamil Nadu, for providing facilities for conducting Research.

FUNDING

No funding was received for this work.

AUTHORS CONTRIBUTIONS

Mohd Abdul Baqi-Conceptualization, validation, writing-original draft preparation, and Data curation. Koppula Jayanthi-Data curation, methodology, writing-Review and Editing. Raman Rajesh Kumar-Conceptualization, Formal analysis, validation and supervision

CONFLICT OF INTERESTS

Declared none

REFERENCES

1. Smith WL, DE Witt DL, Garavito RM. Cyclooxygenases: structural cellular and molecular biology. Annu Rev Biochem. 2000 Jun;69(1):145-82. doi: 10.1146/annurev.biochem.69.1.145, PMID 10966456.
2. Ghosh N, Chaki R, Mandal V, Mandal SC. COX-2 as a target for cancer chemotherapy. Pharmacol Rep. 2010 Mar;62(2):233-44. doi: 10.1016/s1734-1140(10)70262-0, PMID 20508278.
3. Hla T, Neilson K. Human cyclooxygenase-2 cDNA. Proc Natl Acad Sci USA. 1992 Aug 15;89(16):7384-8. doi: 10.1073/pnas.89.16.7384, PMID 1380156.
4. Wang D, DU Bois RN. Eicosanoids and cancer. Nat Rev Cancer. 2010;10(3):181-93. doi: 10.1038/nrc2809, PMID 20168319.
5. Deb PK, Mailabaram RP, Al Jaidi B, Saadh M. Molecular basis of binding interactions of NSAIDs and computer-aided drug design approaches in the pursuit of the development of cyclooxygenase-2 (COX-2) selective inhibitors. Nonsteroidal Anti-Inflamm Drugs. 2017;2:64. doi: 10.5772/Intechopen.68318.
6. Walker EH, Pacold ME, Perisic O, Stephens L, Hawkins PT, Wymann MP. Structural determinants of phosphoinositide 3-kinase inhibition by wortmannin LY294002 quercetin myricetin and staurosporine. Mol Cell. 2000;6(4):909-19. doi: 10.1016/s1097-2765(05)00089-4, PMID 11090628.
7. Gadewar M, Lal B. Molecular docking and screening of drugs for 6lu7 protease inhibitor as a potential target for COVID-19. Int J App Pharm. 2022;14(1):100-5. doi: 10.22159/ijap.2022v14i1.43132.
8. Pant K, Karpel RL, Rouzina I, Williams MC. Mechanical measurement of single molecule binding rates: kinetics of DNA helix destabilization by T4 gene 32 protein. J Mol Biol. 2004;336(4):851-70. doi: 10.1016/j.jmb.2003.12.025, PMID 15095865.
9. Sherman W, Beard HS, Farid R. Use of an induced fit receptor structure in virtual screening. Chem Biol Drug Des. 2006 Jan;67(1):83-4. doi: 10.1111/j.1747-0285.2005.00327.x, PMID 16492153.
10. Harder E, Damm W, Maple J, WU C, Reboul M, Xiang JY. Opls3: a force field providing broad coverage of drug like small molecules and proteins. J Chem Theory Comput. 2016 Jan 12;12(1):281-96. doi: 10.1021/acs.jctc.5b00864, PMID 26584231.
11. Procacci P. Methodological uncertainties in drug-receptor binding free energy predictions based on classical molecular dynamics. Curr Opin Struct Biol. 2021 Apr;67:127-34. doi: 10.1016/j.sbi.2020.08.001, PMID 33220532.
12. Friesner RA, Banks JL, Murphy RB, Halgren TA, Klicic JJ, Mainz DT. Glide: a new approach for rapid, accurate docking and scoring. 1. Method and assessment of docking accuracy. J Med Chem. 2004 Mar 1;47(7):1739-49. doi: 10.1021/jm0306430, PMID 15027865.
13. Jayanthi K, Ahmed SS, Baqi MA, Afzal Azam MA. Molecular docking dynamics of selected benzylidene aminophenyl acetamides as Tmk inhibitors using high throughput virtual screening (Htvs). Int J App Pharm. 2024;16(3):290-7. doi: 10.22159/ijap.2024v16i3.50023.

14. Divyashri G, Krishna Murthy TP, Sundareshan S, Kamath P, Murahari M, Saraswathy GR. In silico approach towards the identification of potential inhibitors from *Curcuma amada Roxb* against H. pylori: ADMET screening and molecular docking studies. Bioimpacts. 2021;11(2):119-27. doi: 10.34172/bi.2021.19, PMID 33842282.
15. Mulakala C, Viswanadhan VN. Could MM-GBSA be accurate enough for calculation of absolute protein/ligand binding free energies? J Mol Graph Model. 2013 Nov;46:41-51. doi: 10.1016/j.jmgm.2013.09.005, PMID 24121518.
16. Cleveland J, Montville TJ, Nes IF, Chikindas ML. Bacteriocins: safe natural antimicrobials for food preservation. Int J Food Microbiol. 2001;71(1):1-20. doi: 10.1016/s0168-1605(01)00560-8, PMID 11764886.
17. Barbosa MS, Todorov SD, Belguesmia Y, Choiset Y, Rabesona H, Ivanova IV. Purification and characterization of the bacteriocin produced by *lactobacillus sakei MBSa1* isolated from Brazilian salami. J Appl Microbiol. 2014;116(5):1195-208. doi: 10.1111/jam.12438, PMID 24506656.
18. Cadieux P, Wind A, Sommer P, Schaefer L, Crowley K, Britton RA. Evaluation of *reuterin* production in urogenital probiotic *lactobacillus reuteri* RC-14. Appl Environ Microbiol. 2008 Aug;74(15):4645-9. doi: 10.1128/AEM.00139-08, PMID 18539802.
19. Aasen IM, Markussen S, Moretro T, Katla T, Axelsson L, Naterstad K. Interactions of the bacteriocins *sakacin P* and *nisin* with food constituents. Int J Food Microbiol. 2003;87(1-2):35-43. doi: 10.1016/s0168-1605(03)00047-3, PMID 12927705.
20. Cahyani RD, Mustopa AZ, Umami RN, Firdaus ME, Manguntungi AB, Arwansyah A. Molecular docking analysis for screening of cyclooxygenase-2 inhibitors from secondary metabolite compounds of *lactococcus lactis subsp. lactis (Lac3)*. Philipp J Sci. 2023;152(4):1307-24. doi: 10.56899/152.04.04.
21. Chaudhary N, Aparoy P. Deciphering the mechanism behind the varied binding activities of COXIBs through molecular dynamic simulations MM-PBSA binding energy calculations and per-residue energy decomposition studies. J Biomol Struct Dyn. 2017 Mar 12;35(4):868-82. doi: 10.1080/07391102.2016.1165736, PMID 26982261.
22. Uzzaman M, Mahmud T. Structural modification of aspirin to design a new potential cyclooxygenase (COX-2) inhibitors. In Silico Pharmacol. 2020;8(1):1. doi: 10.1007/s40203-020-0053-0, PMID 32181121.
23. Pairet M, Engelhardt G. Distinct isoforms (COX-1 and COX-2) of cyclooxygenase: possible physiological and therapeutic implications. Fundam Clin Pharmacol. 1996;10(1):1-17. doi: 10.1111/j.1472-8206.1996.tb00144.x, PMID 8900495.
24. Lipinski CA. Lead and drug-like compounds: the rule of five revolution. Drug Discov Today Technol. 2004;1(4):337-41. doi: 10.1016/j.ddtec.2004.11.007, PMID 24981612.
25. Redhu S, Jindal A. Molecular modelling: a new scaffold for drug design. Int J Pharm Pharm Sci. 2013;5(5).
26. Antao AM, Tyagi A, Kim KS, Ramakrishna S. Advances in deubiquitinating enzyme inhibition and applications in cancer therapeutics. Cancers. 2020;12(6):1579. doi: 10.3390/cancers12061579, PMID 32549302.
27. Zhivkova Z. Quantitative structure pharmacokinetics modeling of the unbound clearance for neutral drugs. Int J Curr Pharm Sci. 2018;10(2):56-9. doi: 10.22159/ijcpr.2018v10i2.25849.
28. R Pounikar A, J Umekar M, R Gupta K. Genotoxic impurities: an important regulatory aspect. Asian J Pharm Clin Res. 2020;13(6):10-25. doi: 10.22159/ajpcr.2020.v13i6.37370.
29. Thiyam R, Narasu ML. Evaluation of cytotoxic and genotoxic effects of zerumbone on colon adenocarcinoma COLO205 cells and human lymphocytes. Int J Pharm Pharm Sci. 2017;9(10):92-6. doi: 10.22159/ijpps.2017v9i11.21120.